COMMUNICATIONS IN NUMERICAL METHODS IN ENGINEERING
*Commun. Numer. Meth. Engng* 2006; **22**:319–333
Published online 6 October 2005 in Wiley InterScience (www.interscience.wiley.com). DOI: 10.1002/cnm.821

# Partitioned formulation of frictional contact problems using localized Lagrange multipliers

José A. González[1], K. C. Park[2,*,†] and Carlos A. Felippa[2]

[1]*Escuela Superior de Ingenieros de Sevilla, Avda. de los Descubrimientos s/n, 41092 Sevilla, Spain*
[2]*Department of Aerospace Engineering Sciences, Center for Aerospace Structures, University of Colorado, Boulder, CO 80309-0429, U.S.A.*

SUMMARY

Interface treatment methods for the contact problem between non-matching meshes have traditionally been based on a direct coupling of the contacting solids employing a master–slave strategy or classical Lagrange multipliers. These methods tend to generate strongly coupled systems that is dependent on the discretization characteristics on each side of the contact zone. In this work a displacement *frame* is intercalated between the interface meshes. The frame is then discretized so that the discrete frame nodes are connected to the contacting substructures using the localized Lagrange multipliers collocated at the interface nodes. The resulting methodology alleviates the need for master–slave book-keeping and provides a partitioned formulation which preserves software modularity, facilitates non-matching mesh treatment and passes the contact patch test. Frictional contact problems are used to demonstrate the salient features of the proposed method. Copyright © 2005 John Wiley & Sons, Ltd.

KEY WORDS: contact; friction; finite element method; localized Lagrange multipliers

## 1. INTRODUCTION

In computational structural mechanics, problems presenting frictional contact surfaces combined with non-matching meshes remain as a difficult task. The source of this difficulty comes not only from the strong non-linearity of the frictional contact law, involving multi-valued relationships between kinematic and static variables, but also from the severe discontinuity

*Correspondence to: K. C. Park, Center for Aerospace Structures and Department of Aerospace Engineering Sciences, University of Colorado at Boulder, Campus Box 429, Boulder, CO 80309-0429, U.S.A.
†E-mail: kcpark@colorado.edu

Contract/grant sponsor: Ministerio de Ciencia y Tecnología; contract/grant number: DPI 2003-00487
Contract/grant sponsor: Consejería de Educación y Ciencia, Junta de Andalucia, Spain. Convocatoria 2004 de concesión de ayudas para el perfeccionamiento de investigadores en centros de investigación fuera de Andalucía

*Received 2 February 2005*
*Revised 25 June 2005*
*Accepted 21 July 2005*

forced by the different meshes used to model the contact interface. Most existing interface treatment methods for the contact problem between non-matching meshes have traditionally been based on a direct coupling of the contacting solids employing a master–slave strategy, classical Lagrange multipliers or mortar-like methods [1–4].

The present work is an extension of the formulation proposed by Rebel *et al.* [5] to solve the contact problem with non-matching meshes introducing an intermediate contact surface, or *contact frame*, endowed with independent degrees of freedom and treated with a FEM discretization. This frame is connected to the contacting substructures using localized Lagrange multipliers [6] and can be constructed in order to preserve the constant–stress interface patch test [7]. In the work of Rebel *et al.* a general formulation of the problem is derived using the variational framework proposed by Park and Felippa [8, 9] and then is particularized to the two-dimensional case. However, they considered the contact zone to be *a priori* known after applying a two stages predictor–corrector algorithm and decided the contact point states using a *trial and error* based algorithm.

In the present work, we extend [5] so that the contact frame may separate from the substructures in all directions, that is, the frame now is a completely free system that moves while maintaining the contact zone as an unknown. Another new feature is in the way of finding contact states; in the present work contact conditions are imposed mathematically using the augmented Lagrangian formulation and projection functions, making the contact search to be part of the overall contact algorithm.

## 2. THE CONTACT FRAME

Let us suppose two solids in contact and denote their domains $\Omega$ and $\bar{\Omega}$. To formulate the contact problem, instead of considering the direct interaction between the two bodies during the contact process, we will insert a deforming non-physical surface $\Lambda$ between them and reformulate the contact problem in terms of interaction of the two solids with this new element, called the *contact frame*, using localized Lagrange multipliers on each side of the frame.

The contact tractions acting on the frame are represented in the exploded view of Figure 1 where the localized Lagrange multipliers connecting solid $\Omega$ with the frame are named using the vector quantity $\boldsymbol{\lambda} = (\lambda_n, \lambda_{t_1}, \lambda_{t_2})^t$ and the multipliers connecting solid $\bar{\Omega}$ are named $\bar{\boldsymbol{\lambda}} = (\bar{\lambda}_n, \bar{\lambda}_{t_1}, \bar{\lambda}_{t_2})^t$. These forces are expressed using two locally orthonormal base systems connected to the frame; $\mathbf{B} = [\mathbf{n}, \mathbf{a}_1, \mathbf{a}_2]$ used to describe $\boldsymbol{\lambda}$ and $\bar{\mathbf{B}} = [\bar{\mathbf{n}}, \bar{\mathbf{a}}_1, \bar{\mathbf{a}}_2]$ used for $\bar{\boldsymbol{\lambda}}$. These local systems for describing the frame kinematics are defined in the following way; $\mathbf{a}_1$ and $\mathbf{a}_2$ are the orthogonal vectors contained in the frame tangent plane at the considered point and vector $\mathbf{n}$ points towards solid $\bar{\Omega}$. The barred base system $\bar{\mathbf{B}}$ at the same position, will be defined in opposite direction to $\mathbf{B}$.

In order to describe the motion of the two solids we use the displacement fields $\mathbf{u}$ and $\bar{\mathbf{u}}$ defined on $\Omega$ and $\bar{\Omega}$, respectively, which when added to the reference configurations $\mathbf{X}$ and $\bar{\mathbf{X}}$, provide us with the current positions $\mathbf{x}$ and $\bar{\mathbf{x}}$

$$\begin{aligned} \mathbf{x} &= \mathbf{X} + \mathbf{u} \\ \bar{\mathbf{x}} &= \bar{\mathbf{X}} + \bar{\mathbf{u}} \end{aligned} \tag{1}$$

 

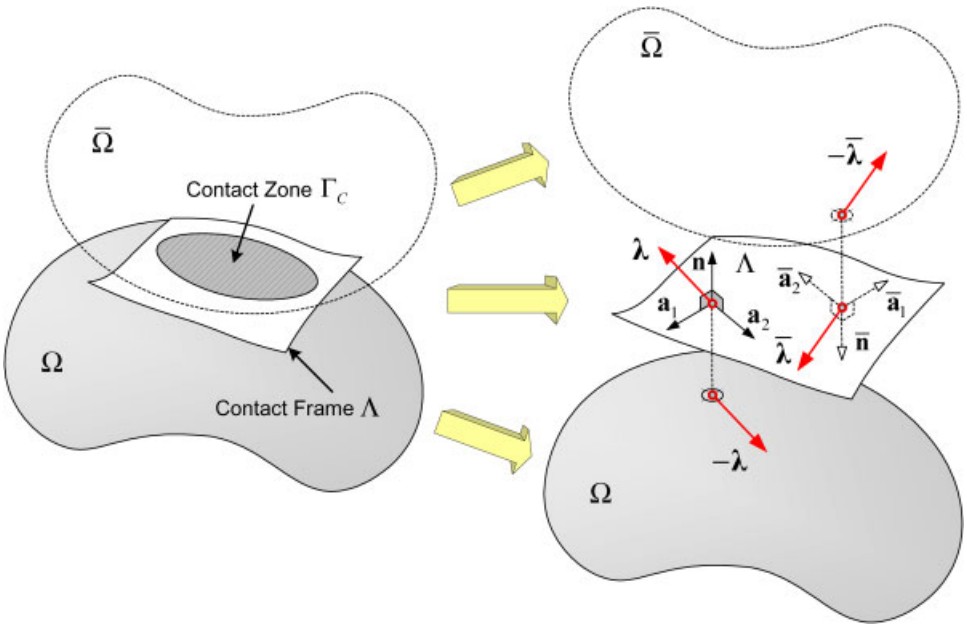


Figure 1. Left: Contact interfaces with intercalated frame. Right: Exploded view with localized Lagrange multipliers.

The motion of the contact frame is described using its displacements $\mathbf{v}$ from its initial configuration $\mathbf{Y}$, providing a current position

$$\mathbf{y} = \mathbf{Y} + \mathbf{v} \tag{2}$$

however, this motion will be restricted to permanently maintain the frame just in the middle between the two contact interfaces. To do that, the relative frame–contact interface distance vectors $\mathbf{k} = (k_n, k_{t_1}, k_{t_2})^t$ and $\bar{\mathbf{k}} = (\bar{k}_n, \bar{k}_{t_1}, \bar{k}_{t_2})^t$ are expressed in a local co-ordinate system of the frame by

$$\begin{aligned} \mathbf{k} &= \mathbf{B}^t(\mathbf{x} - \mathbf{y}) \\ \bar{\mathbf{k}} &= \bar{\mathbf{B}}^t(\bar{\mathbf{x}} - \mathbf{y}) \\ \mathbf{k} - \bar{\mathbf{k}} &= 0 \end{aligned} \tag{3}$$

With previous definitions [5] the contact frame matches the contact zone $\Gamma_c$ where $k_n$ is equal to zero. Also $\mathbf{k}_t$ will give us the direction of the relative motion of the contact interfaces, is a variable needed to formulate the frictional behaviour.

## 3. ENFORCEMENT OF THE CONTACT CONDITIONS

The behaviour of the contact interface is governed by the non-penetration condition and the Coulomb friction law. To formulate the contact conditions, let us introduce the *augmented*

 

*Lagrange multiplier* variable $\boldsymbol{\lambda}(r) = \boldsymbol{\lambda} + r\mathbf{k}$ with a penalty parameter $r > 0$, and the Coulomb disk of radius $g$ projection operator $\mathbb{P}_{\mathbb{C}_g}(.) : \mathbb{R}^2 \to \mathbb{R}^2$

$$\mathbb{P}_{\mathbb{C}_g}(x, y) = \begin{cases} [x, y]^t & \text{if } x^2 + y^2 \leqslant g^2 \\ \dfrac{g}{\sqrt{x^2 + y^2}}[x, y]^t & \text{otherwise} \end{cases} \tag{4}$$

then, the complete fulfilment of contact conditions can be assured using the cone projection operator $\mathbb{P}_{\triangleleft}(.) : \mathbb{R}^3 \to \mathbb{R}^3$ applied to the augmented Lagrangian multipliers in the following way:

$$\mathbb{P}_{\triangleleft}(\boldsymbol{\lambda}(r)) = \begin{bmatrix} \max(0, \lambda_n(r)) \\ \mathbb{P}_{\mathbb{C}_{\mu \max(0, \lambda_n)}}(\boldsymbol{\lambda}_t(r)) \end{bmatrix} \tag{5}$$

This definition allows us to express the contact conditions with the final expression

$$\mathbb{P}_{\triangleleft}(\boldsymbol{\lambda}(r)) = \boldsymbol{\lambda} \tag{6}$$

that permits to satisfy exactly the contact constraints and friction criteria contrary to penalty techniques.

## 4. VARIATIONAL FORMULATION

To derive the equilibrium equations of the constrained system we use the variational formulation proposed by Park and Felippa [8, 9] where the problem is treated as if all bodies were entirely free, formulating the virtual work by summing up the contributions of each body. The localized constraint conditions are constructed and then multiplied by unknown coefficients, denoted herein as the localized Lagrange multipliers. The resulting constraint functional is added to the virtual work of the free substructures to yield the total work of the system.

The variational functional that represents the total energy of the system $\delta\Pi$, is then composed by the energy of the two completely free substructures plus the interface constraint functional associated with the contact phenomena

$$\delta\Pi = \delta\pi^{\text{free}} + \delta\bar{\pi}^{\text{free}} + \delta\pi_i^{\text{total}} \tag{7}$$

where the contact interface potential $\delta\pi_i^{\text{total}}$ consists of contributions from both sides

$$\delta\pi_i^{\text{total}} = \delta\pi_i + \delta\bar{\pi}_i \tag{8}$$

which will be derived in this section.

To do that, let us decompose each one of the two interface functionals into two terms

$$\begin{aligned} \delta\pi_i &= \delta\pi_k + \delta\pi_c \\ \delta\bar{\pi}_i &= \delta\bar{\pi}_k + \delta\bar{\pi}_c \end{aligned} \tag{9}$$

 

the first one is related with the kinematic positioning of the frame, Equation (3), that is enforced in a weak sense using the variational form

$$\delta\pi_k = \iint_{\Gamma_c} (\delta\{\boldsymbol{\lambda}\cdot[\mathbf{B}^t(\mathbf{x}-\mathbf{y})-\mathbf{k}]\})\,\mathrm{d}\Gamma_c \tag{10}$$

and the second one represents the virtual work of the contact forces, contribution to the weak form that can be expressed in the following way:

$$\delta\pi_c = \iint_{\Gamma_c} (\boldsymbol{\lambda}\cdot\delta\mathbf{k})\,\mathrm{d}\Gamma_c \tag{11}$$

where the contact forces $\boldsymbol{\lambda}$ have to satisfy the unilateral contact law and the frictional law. These restrictions can be automatically satisfied replacing the Lagrange multipliers by the projection operator (5) obtaining

$$\delta\pi_c = \iint_{\Gamma_c} (\mathbb{P}_{\lhd}(\boldsymbol{\lambda}(r))\cdot\delta\mathbf{k})\,\mathrm{d}\Gamma_c \tag{12}$$

Substituting (12) and (10) into the first of (9) provides the expression for the total variation of the interface potential at the non-barred side

$$\delta\pi_i = \iint_{\Gamma_c} (\boldsymbol{\lambda}\cdot\delta\{\mathbf{B}^t(\mathbf{x}-\mathbf{y})\}+\delta\boldsymbol{\lambda}\cdot\{\mathbf{B}^t(\mathbf{x}-\mathbf{y})-\mathbf{k}\}+\delta\mathbf{k}\cdot\{-\boldsymbol{\lambda}+\mathbb{P}_{\lhd}(\boldsymbol{\lambda}(r))\})\,\mathrm{d}\Gamma_c \tag{13}$$

Similarly, one can obtain $\delta\bar{\pi}_i$ as

$$\delta\bar{\pi}_i = \iint_{\Gamma_c} (\bar{\boldsymbol{\lambda}}\cdot\delta\{\bar{\mathbf{B}}^t(\bar{\mathbf{x}}-\mathbf{y})\}+\delta\bar{\boldsymbol{\lambda}}\cdot\{\bar{\mathbf{B}}^t(\bar{\mathbf{x}}-\mathbf{y})-\mathbf{k}\}+\delta\mathbf{k}\cdot\{-\bar{\boldsymbol{\lambda}}+\mathbb{P}_{\lhd}(\bar{\boldsymbol{\lambda}}(r))\})\,\mathrm{d}\Gamma_c \tag{14}$$

for the barred side.

To deal with the first terms of Equations (13) and (14) we decompose them in the following way:

$$\boldsymbol{\lambda}\cdot\delta\{\mathbf{B}^t(\mathbf{x}-\mathbf{y})\} = (\delta\mathbf{u}-\delta\mathbf{v})\cdot\{\mathbf{B}\boldsymbol{\lambda}\}+\lambda_n\delta\mathbf{n}\cdot(\mathbf{x}-\mathbf{y})+\lambda_{t_\alpha}\delta\mathbf{a}_\alpha\cdot(\mathbf{x}-\mathbf{y}) \tag{15}$$

$$\bar{\boldsymbol{\lambda}}\cdot\delta\{\bar{\mathbf{B}}^t(\bar{\mathbf{x}}-\mathbf{y})\} = (\delta\bar{\mathbf{u}}-\delta\mathbf{v})\cdot\{\bar{\mathbf{B}}\bar{\boldsymbol{\lambda}}\}+\bar{\lambda}_n\delta\bar{\mathbf{n}}\cdot(\bar{\mathbf{x}}-\mathbf{y})+\bar{\lambda}_{t_\alpha}\delta\bar{\mathbf{a}}_\alpha\cdot(\bar{\mathbf{x}}-\mathbf{y}) \tag{16}$$

where the variation of the normal and tangential frame unitary vectors can be written, see Reference [5], as

$$\delta\mathbf{a}_\alpha = \mathbf{Q}^\alpha\delta\mathbf{v}_{,\alpha},\quad \delta\bar{\mathbf{a}}_\alpha = \bar{\mathbf{Q}}^\alpha\delta\mathbf{v}_{,\alpha} \tag{17}$$

$$\delta\mathbf{n} = \mathrm{e}^{\beta\alpha}(\mathbf{a}_\beta\times\mathbf{I})\mathbf{Q}^\alpha\delta\mathbf{v}_{,\alpha},\quad \delta\bar{\mathbf{n}} = \mathrm{e}^{\beta\alpha}(\bar{\mathbf{a}}_\beta\times\mathbf{I})\bar{\mathbf{Q}}^\alpha\delta\mathbf{v}_{,\alpha} \tag{18}$$

 

Substituting into (13) and (14) leads to the final expression for the interface potentials

$$\delta\pi_i = \iint_{\Gamma_c} (\delta\boldsymbol{\lambda}\cdot\{\mathbf{B}^t(\mathbf{x}-\mathbf{y})-\mathbf{k}\}+(\delta\mathbf{u}-\delta\mathbf{v})\cdot\{\mathbf{B}\boldsymbol{\lambda}\} + \delta\mathbf{v}_{,\alpha}\cdot\{\mathbf{Q}^{\alpha}\boldsymbol{\Phi}_{\alpha}(\mathbf{x}-\mathbf{y})\}+\delta\mathbf{k}\cdot\{-\boldsymbol{\lambda}+\mathbb{P}_{\triangleleft}(\boldsymbol{\lambda}(r))\})\,\mathrm{d}\Gamma_c \tag{19}$$

with $\boldsymbol{\Phi}_{\alpha}=\lambda_{t_{\alpha}}\mathbf{I}+\lambda_n \mathrm{e}^{\alpha\beta}(\mathbf{a}_{\beta}\times\mathbf{I})$, and for the barred: side

$$\delta\bar{\pi}_i = \iint_{\Gamma_c} (\delta\bar{\boldsymbol{\lambda}}\cdot\{\bar{\mathbf{B}}^t(\bar{\mathbf{x}}-\mathbf{y})-\mathbf{k}\}+(\delta\bar{\mathbf{u}}-\delta\mathbf{v})\cdot\{\bar{\mathbf{B}}\bar{\boldsymbol{\lambda}}\} + \delta\mathbf{v}_{,\alpha}\cdot\{\bar{\mathbf{Q}}^{\alpha}\boldsymbol{\Phi}_{\alpha}(\bar{\mathbf{x}}-\mathbf{y})\}+\delta\mathbf{k}\cdot\{-\bar{\boldsymbol{\lambda}}+\mathbb{P}_{\triangleleft}(\bar{\boldsymbol{\lambda}}(r))\})\,\mathrm{d}\Gamma_c \tag{20}$$

with $\bar{\boldsymbol{\Phi}}_{\alpha}=\bar{\lambda}_{t_{\alpha}}\mathbf{I}-\lambda_n \mathrm{e}^{\alpha\beta}(\mathbf{a}_{\beta}\times\mathbf{I})$.

It is important to mention that preceding interface constraint functional will not lead to a standard minimization problem, for the Coulomb disk $\mathbb{C}_g$ inside the cone projection operator (5) is a function of the normal contact through the friction limit $g$ which depends on the solution $\mathbf{u}$. To overcome this difficulty and following Alart and Curnier [10] we have obtained a particular form of *quasi*-variational functional by substituting $g$ by the convex set $\mu\max(0,\lambda_n)$; for this reason, the minimization problem associated with (7) is considered as a *quasi*-variational problem.

## 5. DISCRETE EQUATIONS

The discrete contact problem will be defined in terms of *contact pairs*, i.e. couples formed by a set of interface nodes and its associated frame element. Those contact pairs are established before starting each time step, calculating for every potentially contacting boundary node its nearest frame element and projecting geometrically on it, see Figure 2.

The frame displacements $\mathbf{v}(\xi_1,\xi_2)$ and its average distance to the solids $\mathbf{k}(\xi_1,\xi_2)$ are interpolated using isoparametric finite elements in the following form:

$$\mathbf{v}(\xi_1,\xi_2)=\mathbf{N}(\xi_1,\xi_2)\begin{bmatrix} v_1 \\ \vdots \\ v_{n_f}\end{bmatrix},\quad \mathbf{k}(\xi_1,\xi_2)=\mathbf{N}(\xi_1,\xi_2)\begin{bmatrix} k_1 \\ \vdots \\ k_{n_f}\end{bmatrix} \tag{21}$$

where $n_f$ is the number of nodes in the frame element, and

$$\mathbf{N}(\xi_1,\xi_2)=\begin{bmatrix} N_1 & 0 & 0 & \dots & N_{n_f} & 0 & 0 \\ 0 & N_1 & 0 & \dots & 0 & N_{n_f} & 0 \\ 0 & 0 & N_1 & \dots & 0 & 0 & N_{n_f}\end{bmatrix} \tag{22}$$

is the shape functions approximation matrix.

 

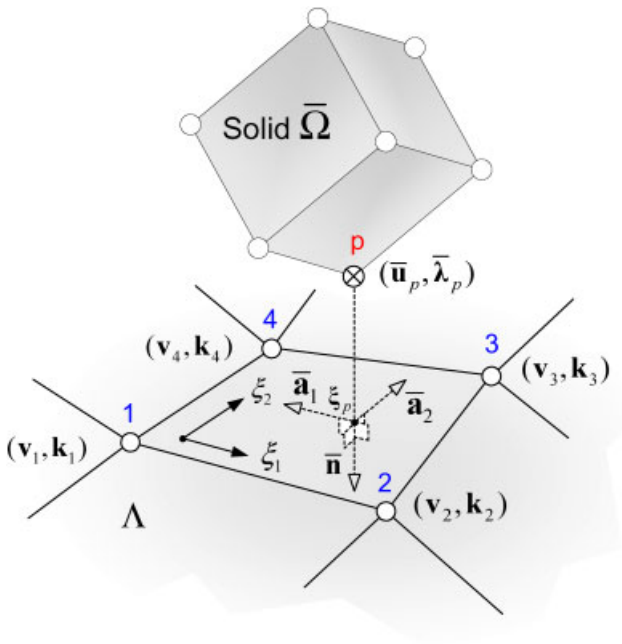


Figure 2. Contact pairs between the barred contact interface node $p$ and the frame. Contact pairs between the non-barred contact interface node and the frame element is independently defined.

The localized Lagrange multipliers are collocated with the contacting interface nodes so that they can be expressed in terms of *Dirac*'*s* delta functions

$$\boldsymbol{\lambda}(\xi_1, \xi_2) = \boldsymbol{\lambda}_p \cdot \delta(\boldsymbol{\xi} - \boldsymbol{\xi}_p) \tag{23}$$

with $\boldsymbol{\xi} = (\xi_1, \xi_2)$ and $\boldsymbol{\xi}_p$ the frame co-ordinates of the node projection, Figure 2. This definition of contact forces will reduce integrations over the contact zone to summations over the contact pairs, i.e.

$$\iint_{\Gamma_c} \boldsymbol{\lambda}(\xi_1, \xi_2) \cdot \mathbf{f}(\xi_1, \xi_2)\, \mathrm{d}\Gamma_c = \sum_{p=1}^{n_p} \boldsymbol{\lambda}_p \cdot \mathbf{f}(\boldsymbol{\xi}_p) \tag{24}$$

with $n_p$ the total number of contact pairs. Expression (24) is useful in order to maintain the contact interface generic, leading to modular coupling software.

To manage the interface discrete variables we introduce the substructural interface nodal indicator $\mathscr{L}$, the well known Boolean finite element assembling operator defined in the following way:

$$\begin{aligned} \mathbf{u}_p &= \mathscr{L}_{up}\mathbf{u}, \quad \boldsymbol{\lambda}_p = \mathscr{L}_{\lambda p}\boldsymbol{\lambda} \\ \mathbf{v}_p &= \mathscr{L}_{vp}\mathbf{v}, \quad \mathbf{k}_p = \mathscr{L}_{kp}\mathbf{k} \end{aligned} \tag{25}$$

where $\mathscr{L}_{\square p}$ is used to extract the variable associated with a contact interface node $p$ from the global $\square$ unknowns vector.

 

Using the preceding definitions, the discrete variational form of the total energy functional can be finally written

$$\delta\Pi = \delta\mathbf{u}\cdot\mathbf{f} + \delta\bar{\mathbf{u}}\cdot\bar{\mathbf{f}} + \delta\boldsymbol{\lambda}\cdot\mathbf{g} + \delta\bar{\boldsymbol{\lambda}}\cdot\bar{\mathbf{g}} - \delta\mathbf{v}\cdot(\mathbf{q}+\bar{\mathbf{q}}) + \delta\mathbf{k}\cdot(\mathbf{p}+\bar{\mathbf{p}}) \tag{26}$$

where

$$\begin{aligned} \mathbf{f} &= \sum_{p=1}^{n_p} \mathscr{L}_{up}^t \mathbf{f}_p, \quad \mathbf{g} = \sum_{p=1}^{n_p} \mathscr{L}_{\lambda p}^t \mathbf{g}_p \\ \mathbf{q} &= \sum_{p=1}^{n_p} \mathscr{L}_{vp}^t \mathbf{q}_p, \quad \mathbf{p} = \sum_{p=1}^{n_p} \mathscr{L}_{kp}^t \mathbf{p}_p \end{aligned} \tag{27}$$

with the corresponding expressions for the barred quantities.

For each contact pairs, the following equations hold:

$$\mathbf{f}_p = \{\mathbf{f}^{\text{int}} - \mathbf{f}^{\text{ext}} + \mathbf{B}\boldsymbol{\lambda}\}_p, \quad \bar{\mathbf{f}}_p = \{\bar{\mathbf{f}}^{\text{int}} - \bar{\mathbf{f}}^{\text{ext}} + \bar{\mathbf{B}}\bar{\boldsymbol{\lambda}}\}_p \tag{28}$$

$$\mathbf{g}_p = \{\mathbf{B}^t(\mathbf{x}-\mathbf{y}) - \mathbf{N}\mathbf{k}\}_p, \quad \bar{\mathbf{g}}_p = \{\bar{\mathbf{B}}^t(\bar{\mathbf{x}}-\mathbf{y}) - \bar{\mathbf{N}}\mathbf{k}\}_p \tag{29}$$

$$\mathbf{q}_p = \{-\mathbf{N}^t\mathbf{B}\boldsymbol{\lambda} + \mathbf{N}_{,\alpha}^t\mathbf{Q}^\alpha\boldsymbol{\Phi}_\alpha(\mathbf{x}-\mathbf{y})\}_p, \quad \bar{\mathbf{q}}_p = \{-\bar{\mathbf{N}}^t\bar{\mathbf{B}}\bar{\boldsymbol{\lambda}} + \bar{\mathbf{N}}_{,\alpha}^t\bar{\mathbf{Q}}^\alpha\bar{\boldsymbol{\Phi}}_\alpha(\bar{\mathbf{x}}-\mathbf{y})\}_p \tag{30}$$

$$\mathbf{p}_p = \{\mathbf{N}^t(-\boldsymbol{\lambda} + \mathbb{P}_\triangleleft(\boldsymbol{\lambda}(r)))\}_p, \quad \bar{\mathbf{p}}_p = \{\bar{\mathbf{N}}^t(-\bar{\boldsymbol{\lambda}} + \mathbb{P}_\triangleleft(\bar{\boldsymbol{\lambda}}(r)))\}_p \tag{31}$$

where Equation (28) represents the equilibrium equation of each substructure (term $-\mathbf{B}\boldsymbol{\lambda}$ are the contact forces expressed in the global system), Equation (29) governs the relative motion between the frame and the substructures, Equation (30) evaluates the forces acting on the frame and Equation (31) imposes the fulfilment of the contact conditions.

The stationary of the above variational equation, viz. $\delta\Pi = 0$, is obtained by solving for the unknown $\mathbf{z} = (\mathbf{u}, \bar{\mathbf{u}}, \boldsymbol{\lambda}, \bar{\boldsymbol{\lambda}}, \mathbf{v}, \mathbf{k})$ the following $B$-differentiable system:

$$\mathbf{F}(\mathbf{z}) = \begin{bmatrix} \mathbf{f} \\ \bar{\mathbf{f}} \\ \mathbf{g} \\ \bar{\mathbf{g}} \\ -\mathbf{q} - \bar{\mathbf{q}} \\ \mathbf{p} + \bar{\mathbf{p}} \end{bmatrix} = 0 \tag{32}$$

where non $F$-differentiability occurs because equation $\mathbf{p} + \bar{\mathbf{p}}$ can present non-linear directional derivatives.

 

The partitioned equations of motion for the frame-based contact problem are obtained from the Jacobian of system (32), that can be expressed as

$$\begin{bmatrix} \mathbf{K} & \mathbf{0} & \mathbf{B} & \mathbf{0} & -\mathbf{L}_v & \mathbf{0} \\ \mathbf{0} & \bar{\mathbf{K}} & \mathbf{0} & \bar{\mathbf{B}} & -\bar{\mathbf{L}}_v & \mathbf{0} \\ \mathbf{B}^t & \mathbf{0} & \mathbf{0} & \mathbf{0} & -\mathbf{L}_b & -\mathbf{N}_k \\ \mathbf{0} & \bar{\mathbf{B}}^t & \mathbf{0} & \mathbf{0} & -\bar{\mathbf{L}}_b & -\bar{\mathbf{N}}_k \\ -\mathbf{L}_v^t & -\bar{\mathbf{L}}_v^t & -\mathbf{L}_b^t & -\bar{\mathbf{L}}_b^t & -\mathbf{D}_v - \bar{\mathbf{D}}_v & \mathbf{0} \\ \mathbf{0} & \mathbf{0} & \mathbf{P}_\lambda & \bar{\mathbf{P}}_\lambda & \mathbf{0} & \mathbf{P}_k + \bar{\mathbf{P}}_k \end{bmatrix} \begin{bmatrix} \Delta\mathbf{u} \\ \Delta\bar{\mathbf{u}} \\ \Delta\boldsymbol{\lambda} \\ \Delta\bar{\boldsymbol{\lambda}} \\ \Delta\mathbf{v} \\ \Delta\mathbf{k} \end{bmatrix} = \begin{bmatrix} -\mathbf{f} \\ -\bar{\mathbf{f}} \\ -\mathbf{g} \\ -\bar{\mathbf{g}} \\ \mathbf{q} + \bar{\mathbf{q}} \\ -\mathbf{p} - \bar{\mathbf{p}} \end{bmatrix} \tag{33}$$

where only non-differentiable terms $\mathbf{P}_\lambda$, $\bar{\mathbf{P}}_\lambda$, $\mathbf{P}_k$ and $\bar{\mathbf{P}}_k$ need a special treatment.

For example, components of the preceding equation for the non-barred quantities are obtained by assembling contributions of each contact pairs $p$

$$\begin{aligned} \mathbf{B} &= \sum_{p=1}^{n_p} \mathscr{L}_{up}^t \mathbf{B}_p \mathscr{L}_{\lambda p}, \quad \mathbf{L}_v = \sum_{p=1}^{n_p} \mathscr{L}_{up}^t \mathbf{L}_{vp} \mathscr{L}_{vp} \\ \mathbf{L}_b &= \sum_{p=1}^{n_p} \mathscr{L}_{\lambda p}^t \mathbf{L}_{bp} \mathscr{L}_{vp}, \quad \mathbf{N}_k = \sum_{p=1}^{n_p} \mathscr{L}_{\lambda p}^t \mathbf{N}_{kp} \mathscr{L}_{kp} \\ \mathbf{D}_v &= \sum_{p=1}^{n_p} \mathscr{L}_{vp}^t \mathbf{D}_{vp} \mathscr{L}_{vp} \\ \mathbf{P}_\lambda &= \sum_{p=1}^{n_p} \mathscr{L}_{kp}^t \mathbf{P}_{\lambda p} \mathscr{L}_{\lambda p}, \quad \mathbf{P}_k = \sum_{p=1}^{n_p} \mathscr{L}_{kp}^t \mathbf{P}_{kp} \mathscr{L}_{kp} \end{aligned} \tag{34}$$

with sums extended to the $n_p$ contact pairs from that side and where each term comes from differentiation of Equations (28)–(29)

$$\mathbf{L}_{vp} = \{-\boldsymbol{\Phi}_\alpha^t \mathbf{Q}^\alpha \mathbf{N}_{,\alpha}\}_p \tag{35}$$

$$\mathbf{L}_{bp} = \left\{ \mathbf{B}^t \mathbf{N} - \begin{bmatrix} -(\mathbf{x}-\mathbf{y})^t(\mathbf{a}_2 \times \mathbf{I}) \\ (\mathbf{x}-\mathbf{y})^t \\ \mathbf{0} \end{bmatrix} \mathbf{Q}^1 \mathbf{N}_{,1} - \begin{bmatrix} (\mathbf{x}-\mathbf{y})^t(\mathbf{a}_1 \times \mathbf{I}) \\ \mathbf{0} \\ (\mathbf{x}-\mathbf{y})^t \end{bmatrix} \mathbf{Q}^2 \mathbf{N}_{,2} \right\}_p \tag{36}$$

$$\mathbf{N}_{kp} = \{\mathbf{N}\}_p \tag{37}$$

$$\mathbf{D}_{vp} = \left\{ \begin{array}{l} \mathbf{N}^t[\boldsymbol{\Phi}_\alpha^t \mathbf{Q}^\alpha]\mathbf{N}_{,\alpha} + \mathbf{N}_{,\alpha}^t[\mathbf{Q}^\alpha \boldsymbol{\Phi}_\alpha]\mathbf{N} + \mathbf{N}_{,\alpha}^t \dfrac{1}{\|\mathbf{y}_{,\alpha}\|} \\ \quad \times \{\mathbf{Q}^\alpha \boldsymbol{\Phi}_\alpha(\mathbf{x}-\mathbf{y}) \otimes \mathbf{a}_\alpha + \mathbf{a}_\alpha \otimes \mathbf{Q}^\alpha \boldsymbol{\Phi}_\alpha(\mathbf{x}-\mathbf{y}) \\ \quad + [\boldsymbol{\Phi}_\alpha(\mathbf{x}-\mathbf{y})] \cdot \mathbf{a}_\alpha \mathbf{Q}^\alpha\} \mathbf{N}_{,\alpha} \end{array} \right\}_p \tag{38}$$

Expressions for the barred side can be similarly obtained.

 

On the other hand, terms $\mathbf{P}_{\boldsymbol{\lambda} p}$ and $\bar{\mathbf{P}}_{\boldsymbol{\lambda} p}$ are decomposed into their normal and tangential parts

$$\mathbf{P}_{\lambda p} = \mathbf{P}_{\lambda_n p} + \mathbf{P}_{\lambda_t p} \quad \text{and} \quad \mathbf{P}_{k p} = \mathbf{P}_{k_n p} + \mathbf{P}_{\lambda_t p} \tag{39}$$

with the following definition for the normal part:

1. Case $\lambda_n(r) < 0$

$$\mathbf{P}_{\lambda_n p} = \left\{ \mathbf{N}^t \begin{bmatrix} -1 & 0 & 0 \\ 0 & 0 & 0 \\ 0 & 0 & 0 \end{bmatrix} \right\}_p$$

2. Case $\lambda_n(r) \geqslant 0$

$$\mathbf{P}_{k_n p} = \left\{ \mathbf{N}^t \begin{bmatrix} r & 0 & 0 \\ 0 & 0 & 0 \\ 0 & 0 & 0 \end{bmatrix} \mathbf{N} \right\}_p$$

In the preceding equations one can see that instead of calculating a complicated non-linear directional derivative for the non-differentiable case $\lambda_n(r) = 0$, it has been replaced by a more simple linear derivative coming from the right side. A similar technique is used for non-differentiable points of the tangential contribution:

1. Case $\lambda_n \leqslant 0$

$$\mathbf{P}_{\lambda_t p} = \left\{ \mathbf{N}^t \begin{bmatrix} 0 & 0 & 0 \\ 0 & -1 & 0 \\ 0 & 0 & -1 \end{bmatrix} \right\}_p$$

2. Case $\lambda_n > 0$

   (a) When $\|\boldsymbol{\lambda}_t(r)\| \leqslant \mu \lambda_n$

$$\mathbf{P}_{k_t p} = \left\{ \mathbf{N}^t \begin{bmatrix} 0 & 0 & 0 \\ 0 & r & 0 \\ 0 & 0 & r \end{bmatrix} \mathbf{N} \right\}_p$$

   (b) otherwise, if $\|\boldsymbol{\lambda}_t(r)\| > \mu \lambda_n$

$$\mathbf{P}_{\lambda_t p} = \left\{ \mathbf{N}^t \begin{bmatrix} 0 & 0 & 0 \\ \alpha \dfrac{\lambda_{t_1}(r)}{\lambda_n} & \Psi_{11} & \Psi_{12} \\ \alpha \dfrac{\lambda_{t_2}(r)}{\lambda_n} & \Psi_{21} & \Psi_{22} \end{bmatrix} \right\}_p$$

 

$$\mathbf{P}_{k_t p} = \left\{ \mathbf{N}^t \begin{bmatrix} 0 & 0 & 0 \\ 0 & r\Theta_{11} & r\Theta_{12} \\ 0 & r\Theta_{21} & r\Theta_{22} \end{bmatrix} \mathbf{N} \right\}_p$$

with $\alpha = \mu\lambda_n/(\sqrt{\lambda_{t_1}^2(r) + \lambda_{t_2}^2(r)})$, $\beta = \mu\lambda_n/(\lambda_{t_1}^2(r) + \lambda_{t_2}^2(r))^{3/2}$, $\mathbf{\Psi} = (\alpha - 1)\mathbf{I} - \beta\mathbf{R}$, $\mathbf{\Theta} = \alpha\mathbf{I} - \beta\mathbf{R}$ and $\mathbf{R} = \boldsymbol{\lambda}_t(r) \otimes \boldsymbol{\lambda}_t(r)$.

In the above expressions we are using a linearized substitute for the non-linear directional derivative appearing when any of these equalities hold $\lambda_n = 0$, $\lambda_n(r) = 0$ or $\|\boldsymbol{\lambda}_t(r)\| = \mu\lambda_n$, although the function can be expected to be normally differentiable in the large majority of practical cases.

## 6. SOLVING THE NON-LINEAR SYSTEM

To solve system (32) the Generalized Newton's Method with Line Search (GNMLS) has been used. GNMLS is an effective extension of the Newton's method for *B*-differentiable functions proposed by Pang [11] in a general context and particularized by Alart [12] and Christensen [13] for the contact case. This method is based on the computation of the non-linear directional derivative of the objective function; however, it is well known that in contact problems this non-linear directional derivative rarely needs to be computed and can be substituted by a linearized version without affecting the algorithm convergence; this is the approach adopted herein in obtaining (39).

If we define the scalars $\beta \in (0,1)$, $\sigma \in (0,1/2)$, and $\varepsilon > 0$ but small, the application of GNMLS algorithm to solve the non-linear equations $\mathbf{F}(\mathbf{z}) = 0$, can be summarized in the following steps:

1. Time integration $t$: Solve for $\mathbf{z}^{t+\Delta t}$ with the known state variable vector $\mathbf{z}^t$.
   (a) Inner GNMLS iterations, loop $k$.
   (b) Use GMRES to solve for $\Delta\mathbf{z}_k^t$ in the system $\partial\mathbf{F}(\mathbf{z}_k^t; \Delta\mathbf{z}_k^t) = -\mathbf{F}(\mathbf{z}_k^t)$.
   (c) Obtain first integer $m = 1, 2, \ldots$ that fulfills $\mathbf{H}(\mathbf{z}_k^t + \beta^m\Delta\mathbf{z}_k^t) \leqslant (1 - 2\sigma\beta^m)\mathbf{H}(\mathbf{z}_k^t)$ with $\mathbf{H}(\mathbf{z}) = \frac{1}{2}\mathbf{F}^t(\mathbf{z})\mathbf{F}(\mathbf{z})$.
   (d) Update the solution $\mathbf{z}_{k+1}^t = \mathbf{z}_k^t + \tau_k\Delta\mathbf{z}_k^t$ with $\tau_k = \beta^m$.
   (e) If $\mathbf{H}(\mathbf{z}_{k+1}^t) \leqslant \varepsilon$ continue, else compute new GNMLS iteration $k \leftarrow k + 1$.
2. Make $\mathbf{z}^{t+\Delta t} = \mathbf{z}_{k+1}^t$ and solve for next time step $t \leftarrow t + \Delta t$.

The algorithm uses two nested loops, the external one cares for time marching and the internal loop does the Newton subiterations. On each one of these subiterations a linear system has to be solved to compute the search direction, where we use a sparse matrix storage scheme combined with the GMRES solver. When a direction $\Delta\mathbf{z}_k^t$ is obtained, it is scaled by a factor of $\tau_k$ obtained from the decreasing error condition given by (c).

## 7. APPLICATIONS

The problem considered is the Hertzian contact of two geometrically identical elastic spheres of radius $R_1 = R_2 = 8$ mm indented applying an external load $P = 1$ N normal to the contact

 

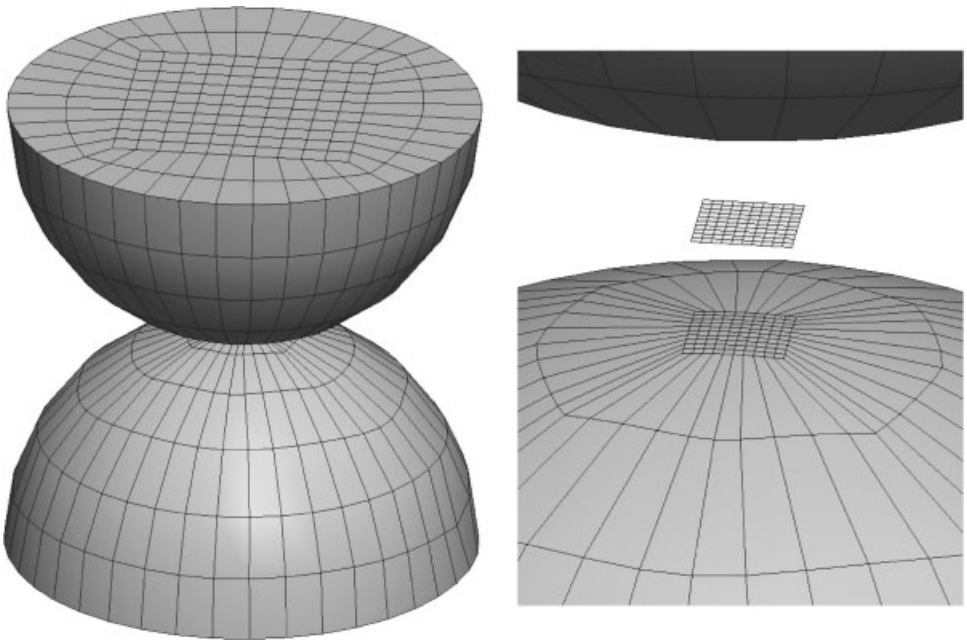

Figure 3. Mesh and frame used for the Hertzian problem.

zone. The material properties for the first sphere are $E_1 = 100\,\text{GPa}$, $v_1 = 0.2$ and $E_2 = 100\,\text{GPa}$, $v_2 = 0.4$ for the second. This difference in the Poisson's ratio, together with a friction coefficient $\mu = 0.25$ will produce a distribution of tangential stresses in the contact zone that will not affect considerably the normal pressure, which will be very close to the Hertz solution that predicts a contact zone radius of 0.378 mm.

The meshes for both spheres are completely identical, generated using 1280 hexahedral elements and 1569 nodes for each one of them, and refining the potentially contact zone (a square of $1\,\text{mm}^2$) with 100 quadrilateral elements and 121 contact nodes, see Figure 3. The contact frame is a plane of $1\,\text{mm}^2$ that uses the same discretization as the potential contact zone and the normal load is applied using ten time steps. It should be noted that because Poisson's ratios for the two contacting spheres are different, the initially matching interface meshes will lead to non-matching meshes.

The convergence rate for one step solution is presented in Figure 4 in terms of relative error $\mathbf{H}(\mathbf{z}^k)/\mathbf{H}(\mathbf{z}^1)$ for each GNMLS subiteration $k$ together with the scaling parameter $\tau_k$. On the right side of the same figure is shown the normal distance from the frame to the spheres in the deformed state where the contact zone is defined by $k_n \approx 0$ and with the mesh resolution used its radius is estimated to be around 0.35 mm.

The normal Lagrange multipliers are presented in Figure 5 compared with the Hertz solution (right) for three cross sections along the $x$ direction. The maximum normal Lagrange multiplier $\lambda_{n\,\max} = 0.035\,\text{N}$ is obtained at the centre of the contact zone and the differences between the numerical results and the Hertz solution can be attributed to a coarse

 

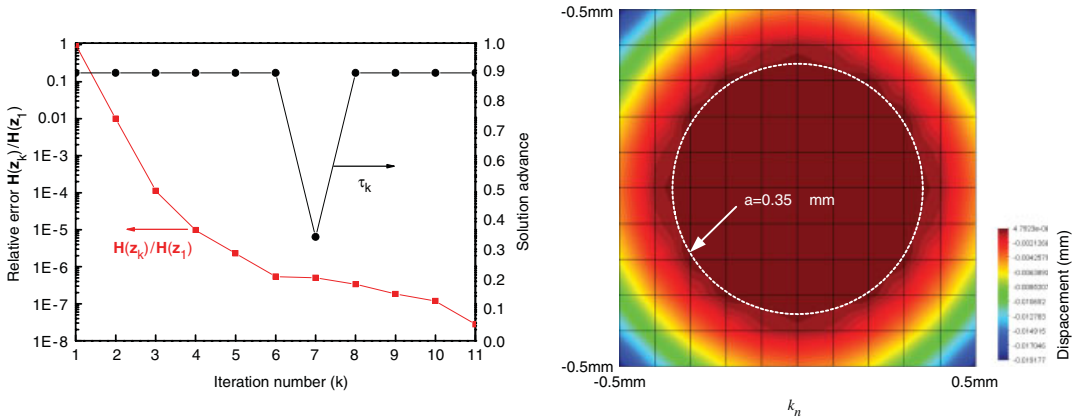


Figure 4. Convergence rate of the GNMLS algorithm and normal distance $k_n$ between the deformed spheres and the frame.

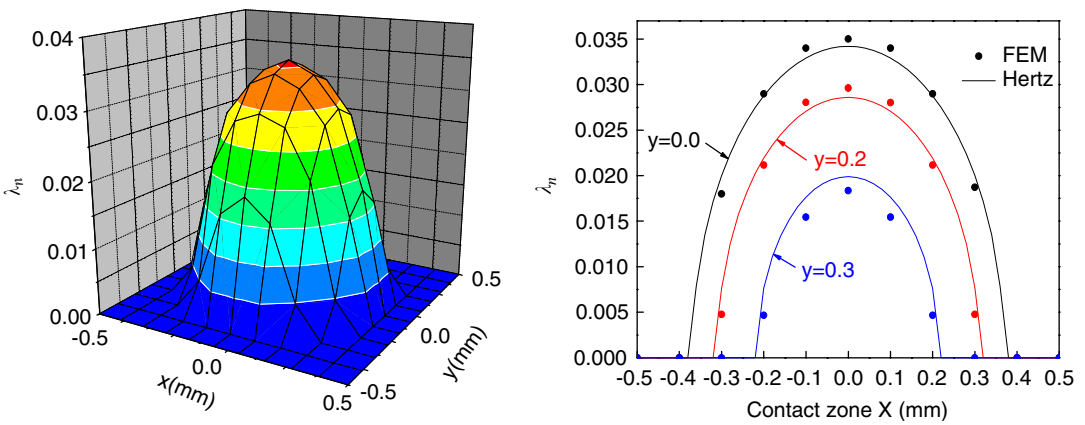


Figure 5. Distribution of normal multipliers in the contact zone and comparison with Hertz solution.

discretization combined with the use of linear elements. It is well known that the coupling between the normal and tangential stresses for this problem is very low, meaning that normal tractions are not considerably affected by the frictional phenomena. It was also observed that the number of steps used to apply the normal load did not modify the normal solution but affected considerably the tangential multipliers inside the central stick zone.

Finally, the tangential Lagrange multipliers in $x$ direction can be seen in Figure 6 obtaining the same solution rotated 90° for the orthogonal direction $y$. It represents a complex shape that has to satisfy the slip condition at the external annular region making the tangential forces equal to the friction limit.

 

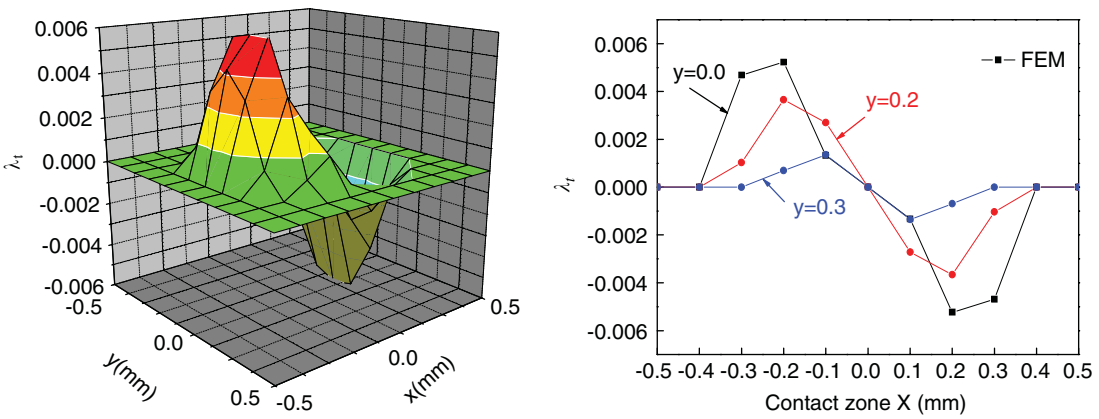


Figure 6. Distribution of tangential multipliers with $\mu = 0.25$ and the normal load $N$ applied with ten time steps.

## 8. CONCLUSION

A formulation of the frictional contact problem using localized Lagrange multipliers to connect the contacting substructures to an adaptative contact frame is presented. The contact conditions are mathematically formulated using projection functions and the contact frame is allowed to move freely between the substructures maintaining the contact zone as an unknown. The GNMLS is applied to solve the non-smooth system of equations representing the equations of motion and different regularization techniques to improve convergence are proposed and tested.

The algorithm and introduced formulations prove to be very robust and efficient when solving 3D non-matching contact problems. Suggested methodology simplifies the procedure to solve these kind of problems, minimizing geometrical knowledge of the contacting substructures needed to formulate the contact interface behaviour. This fact can facilitate further extensions for contact problems, like iterative parallel computations or connection between different numerical techniques like the FEM and the Boundary Element Method.

## REFERENCES

1. Simo JC, Wriggers P, Taylor RL. A perturbed Lagrangian formulation for the finite element solution of contact problems. *Computer Methods in Applied Mechanics and Engineering* 1985; **50**:163–180.
2. Papadopoulos P, Taylor RL. A mixed formulation for the finite element solution of contact problems. *Computer Methods in Applied Mechanics and Engineering* 1992; **94**:373–384.
3. Simo JC, Laursen TA. An augmented Lagrangian treatment of contact problems involving friction. *Computers and Structures* 1992; **42**:97–116.
4. Puso MA, Laursen TA. A mortar segment-to-segment contact method for large deformation solid mechanics. *Computer Methods in Applied Mechanics and Engineering* 2004; **193**:601–629.
5. Rebel G, Park KC, Felippa CA. A contact formulation based on localized Lagrange multipliers: formulation and application to two-dimensional problems. *International Journal for Numerical Methods in Engineering* 2002; **54**(2):263–297.
6. Park KC, Felippa CA, Gumaste UA. A localized version of the method of Lagrange multipliers and its applications. *Computational Mechanics* 2000; **24**:476–490.
7. Park KC, Felippa CA, Rebel G. A simple algorithm for localized construction of non-matching structural interfaces. *International Journal for Numerical Methods in Engineering* 2002; **53**:2117–2142.

 

8. Park KC, Felippa CA. A variational framework for solution method developments in structural mechanics. *Journal of Applied Mechanics* 1998; **65**:242–249.
9. Park KC, Felippa CA. A localized version of the method of Lagrange multipliers and its applications. *Computational Mechanics* 2000; **24**:476–490.
10. Alart P, Curnier A. A mixed formulation for frictional contact problems prone to Newton like solution methods. *Computer Methods in Applied Mechanics and Engineering* 1991; **32**:353–475.
11. Pang JS. Newton's method for *B*-differentiable equations. *Mathematics of Operations Research* 1990; **15**(2):311–341.
12. Alart P. Méthode de Newton généralisée en mécanique du contact. *Journal de Mathematiques Pures et Appliquees* 1997; **76**:83–108.
13. Christensen PW, Klarbring A, Pang JS, Strömberg N. Algorithms for frictional contact problems based on mathematical programming. Linköping University, Sweden, 1998.

 